ISOLATED SINGULARITIES OF A MONGE-AMPÈRE METRIC IN DIMENSION TWO

NEIL PATRAM AND BEN SCOTT

Abstract. We address the regularity of a Monge-Ampère metric g on the surface of a simplex constructed in the recent work [5] by realizing it as a special Käher metric. Supposing that the holomorphic cubic form attached to g does not have an essential singularity and that we can make a choice of isothermal coordinates with sufficient regularity around the origin, we are afforded an exhaustive family of models as proved by Haydys in [4]. These models enable us to conclude in all but a single special case that the potential φ of g fails to be $C^{1,1}$ at the origin. As an accompaniment to this result, we provide numerical simulations of φ, which give insight into the specific model which g should obey.

Contents

1. Introduction

The problem of constructing a Monge-Ampère metric on an singular affine manifold has motivations in the field of mirror symmetry, specifically the SYZ conjecture. This problem was addressed in [5] for the case of the surface of an n-dimensional simplex, where it was demonstrated that the potential φ of the metric g also solves the classical Monge-Ampère equation in Euclidean space through any flat chart.

We restrict ourselves to the case of $n = 3$. In this case, we construct a planar problem in which the singular set consists of a single point. The aforementioned pullback property allows us to consider the planar Monge-Ampère metric $g = \varphi_{xx}\ dx^2 + 2\varphi_{xy}\ dxdy + \varphi_{yy}\ dy^2$ in local affine coordinates (x, y). Then

changing to a specific isothermal coordinate $z = u + iv$ gives $g = e^{-\rho}|dz|^2$, $\rho = \log(2\varphi_{xx} + 4\varphi_{xy} + 2\varphi_{yy})$, as a metric on a domain $\Omega \subseteq \mathbb{C}$ with the topology of the punctured disc. We attach a so-called *special Kähler structure* to the metric g. If ρ can be demonstrated to be sufficiently regular, and the holomorphic cubic form of g does not have an essential singularity, then we may apply [4, Theorem 1.1] and conclude the following.

Theorem 1.1. *Suppose the conformal factor ρ is C^2 on a punctured disk around the origin and the holomorphic cubic form Ξ has order $n > -\infty$ at the origin. Then*

$$e^{-\rho} = -|z|^{n+1}\log|z|e^{O(1)}$$

or

$$e^{-\rho} = |z|^{\beta}(C + o(1)),\ \ \beta < n+1, \beta \neq 0.$$

Moreover, $|D^2\varphi|$ is unbounded near the origin.

In sections 2 and 3, we provide background for Theorem 1.1 and detail our choice of coordinates and special Kähler structure on the domain Ω. In section 4, we provide numerical simulations of the metric to conjecture the correct model.

Finally, in the appendix we give an extended discussion of Theorem 1.1. Specifically, we describe heuristic arguments for the assumptions on ρ and Ξ, as well as for ruling out the possibility of $\beta = 0$ in Theorem 1.1.

2. Singular Monge-Ampère metrics in dimension two

2.1. **Geometric setting.** In this paper we consider the singularities of the solution to an optimal transport problem between the boundary of a tetrahedron and the boundary of its dual, considered as 2-dimensional submanifolds of $\mathbb{R}^3$ and $(\mathbb{R}^3)^*$, respectively.

More specifically, we consider the following points in $\mathbb{R}^3$:

$$m_0 = (1,1,1) \qquad m_1 = (-3,1,1)$$
$$m_2 = (1,-3,1) \qquad m_3 = (1,1,-3)$$

Following the notation of [5], let Δ be the convex hull of these points, and $\Delta^\vee \subseteq (\mathbb{R}^3)^*$ be the dual tetrahedron defined by

$$\Delta^\vee = \{n \in (\mathbb{R}^3)^* : \sup_{m\in\Delta}\langle m, n\rangle = \max_{0\leq i\leq 3}\langle m_i, n\rangle \leq 1\}$$

One may easily check that $\Delta^\vee$ is the convex hull of the following points:

$$n_0 = (-1,-1,-1) \qquad n_1 = (1,0,0)$$
$$n_2 = (0,1,0) \qquad n_3 = (0,0,1)$$

We additionally define $A = \partial\Delta, B = \partial\Delta^\vee$.

Let τ_i denote the face of A opposite m_i; more precisely this is the convex hull of the points $\{m_j : j \neq i\}$. Define σ_i similarly on B.

Also define $S_i \subseteq A$ to be the following set:

$$S_i = \{m \in A : \langle m, n_i\rangle = \min_j \langle m, n_j\rangle\}$$

We define T_i similarly on B. The region T_i may be described in terms of the barycenters of the faces which meet at m_i and the midpoints of the edges which meet at m_i, as shown in Figure 1.

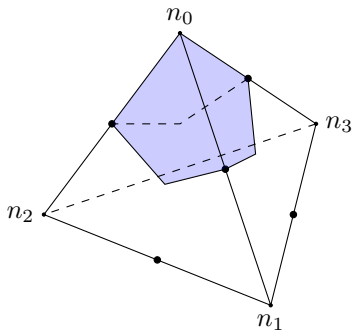

FIGURE 1. A visual depiction of the region T_0 on B

We now equip A and B with the structure of a singular affine manifold via the following charts from [5]. For distinct $i, j, k, l \in \{1, 2, 3, 4\}$, define coordinate charts $p_{i,j}^{-1}$ of A, and coordinates $q_{i,j}^{-1}$ of B by

$$p_{i,j}^{-1}(m) := (\langle m, n_j - n_k\rangle, \langle m, n_j - n_l\rangle)$$
$$q_{i,j}^{-1}(n) := -\frac{1}{4}(\langle n, m_j - m_k\rangle, \langle n, m_j - m_l\rangle)$$

Denote by $L^\infty(A)$ and $L^\infty(B)$ the spaces of bounded real valued functions on A and B, respectively. Given $\varphi \in L^\infty(A), \psi \in L^\infty(B)$, we may define their c-transforms as follows:

$$L^\infty(B) \ni \varphi^c := \sup_{m\in A} \langle m, n\rangle - \varphi(m)$$
$$L^\infty(A) \ni \psi^c := \sup_{n\in B} \langle m, n\rangle - \psi(n)$$

We have that φ^c, ψ^c are bounded due to the fact that A and B (and thus the functionals $\langle \cdot, n\rangle$ and $\langle m, \cdot\rangle$) are bounded. A function $\varphi \in L^\infty(A)$ is called c-convex if $\varphi^{cc} = \varphi$, and similarly for functions $\psi \in L^\infty(B)$.

Given a c-convex function $\psi \in L^\infty(B)$, we define its c-subgradient as the multi-valued map $\partial^c\psi : B \to A$ given by

$$(\partial^c\psi)(n) := \{m \in A : \psi(n) + \psi^c(m) = \langle m, n\rangle\}$$

Now we may put finite measures μ, ν on A and B, respectively, and consider the transport problem between them. It is of interest to the authors of [5] as to the regularity of c-convex functions $\psi \in L^\infty(B)$ such that $(\partial^c\psi^c)_*\mu = \nu$, specifically in the case when μ and ν are Lebesgue measure on their respective tetrahedra. As Lebesgue measure is symmetric with respect to the symmetries of the tetrahedron, we conclude by their Theorem 5.2 that the function ψ is symmetric as well.

2.2. **Connection to planar optimal transport.** In this section we formulate an appropriate planar problem based on the tetrahedral case, with the singularity in the interior of the source domain. In particular, we will attempt to formulate a planar problem analogous to the problem pictured in Figure 2.

Adopting the notation $n_{ij} = \frac{n_i+n_j}{2}, n_{ijk} = \frac{n_i+n_j+n_k}{3}$, we may describe these regions specifically as $A\cap\text{conv}(n_0, n_{013}, n_1, n_{123})$ and $B\cap\text{conv}(m_{123}, m_2, m_{023}, m_0)$;

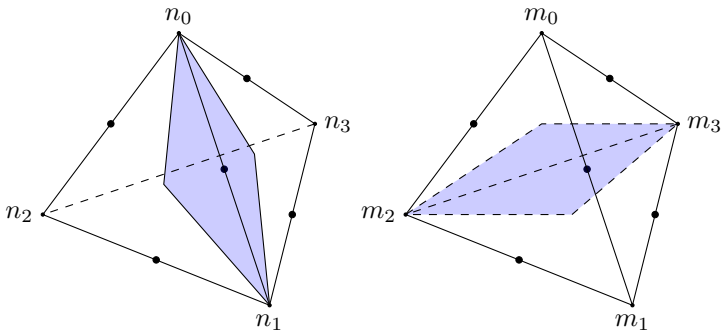

FIGURE 2. Regions of the tetrahedron from which a planar transport problem will be derived

it may be verified by [5, Lemma 4.1] that any bounded symmetric c-convex function must map this region on A into the corresponding region on B.

Given a function ψ on B we may define functions $\psi_{i,j} := (\psi - m_j) \circ q_{i,j}$ which can be thought of as the image of ψ under the charts. The following lemma of [5] determines the c-subgradient images correctly relate the subgradient images of ψ and ψ_{ij}.

Lemma 2.1. [5, Lemma 4.4] *Suppose that ψ is a bounded and symmetric real-valued c-convex function on B. If $i \neq j$, then $p_{j,i}^{-1}$ gives a bijection of $(\partial^c \psi)(n)$ onto $\partial \psi_{i,j}(q_{i,j}^{-1}(n))$ for any $n \in T_i^\circ$. The same result holds for any $n \in \tau_j^\circ$.*

Consider the region formed from the intersecion of B with the convex hull of the points $n_0, n_{012}, n_{01}, n_{013}$, which lies entirely within the region T_0. By Lemma 2.1, using the projection $q_{0,1}^{-1}$, we have that the corresponding planar transport occurs between the convex hull of the points $(0,0), (\frac{1}{3}, 0), (0, \frac{1}{3}), (\frac{1}{2}, \frac{1}{2})$, and the triangular region with vertices $(1,0), (0,1), (\frac{1}{2}, \frac{1}{2})$.

Now we wish to extend our transport problem by appending the triangular region on the tetrahedron bounded by n_{012}, n_1, n_{12} through the chart q_{01}^{-1}. One can calculate that this yields the triangular region in the plane with vertices $(0, \frac{1}{3}), (\frac{1}{2}, \frac{1}{2}), (1,1)$. Denote this region by P.

We wish to find the image of P under the subgradient of ψ_{01}. Lemma 2.1 does not account for this case; however, we may deduce the correct region by relating ψ_{01} to another function obtained by projecting ψ to the plane. Below we will consider ψ_{02}, applying Lemma 2.1 for the case $n \in \tau_2$.

Recall by the definition of ψ_{ij} that we have

$$\psi_{01} = (\psi - n_1) \circ q_{01} \qquad \psi_{02} = (\psi - n_2) \circ q_{02}$$

We now note

$$\psi_{01} \circ q_{01}^{-1}(n) + \langle m_1, n \rangle = \psi_{02} \circ q_{02}^{-1}(n) + \langle m_2, n \rangle$$
$$\psi_{01} \circ q_{01}^{-1}(n) = \psi_{02} \circ q_{02}^{-1}(n) + \langle m_2 - m_1, n \rangle$$

And assigning $n' := q_{01}^{-1}(n)$ yields

$$\psi_{01}(n') = \psi_{02} \circ q_{02}^{-1} \circ q_{01}(n') + \langle m_2 - m_1, q_{01}(n') \rangle$$

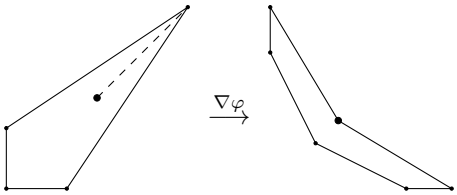

FIGURE 3. The domain Ω and its image under the transport map $\nabla\varphi$

One may check that on the triangle P, $q_{02}^{-1} \circ q_{01}$ is a linear transformation, given by

$$q_{02}^{-1} \circ q_{01} = \begin{bmatrix} -1 & 0 \\ -1 & 1 \end{bmatrix}$$

One may additionally check that

$$\langle m_1 - m_2, q_{01}(n') \rangle = \begin{bmatrix} 1 & 0 \end{bmatrix} n'$$

Now by using the chain rule we may find that

$$\partial\psi_{01} = \begin{bmatrix} -1 & -1 \\ 0 & 1 \end{bmatrix} \partial\psi_{02} + \begin{bmatrix} 1 \\ 0 \end{bmatrix}$$

And the resulting image of P is the triangle with vertices $(\frac{1}{2}, \frac{1}{2}), (1, 0)$, and $(\frac{4}{3}, 0)$.

We also need a parallel result for the region bounded by n_{013}, n_1, n_{13} under ψ_{03} with $n \in \tau_3$. This follows similarly, yielding the triangle with vertices $(\frac{1}{2}, \frac{1}{2}), (0, 1)$, and $(0, \frac{4}{3})$. The transport regions are depicted visually in Figure 2.2. We include a dashed line in the source domain to indicate that this line is not contained in the chart centered at n_0.

3. Models of conformal special Kähler metrics in the plane

The results obtained in [4] and [1] suggest that we might obtain asymptotic behavior at the singular set by viewing our metric as a *special Kähler metric* and working in isothermal coordinates for g. In this section we review some necessary definitions and equip our domain with a special Kähler structure. Then we describe the result which is of primary interest for our application.

3.1. Special Kähler structure.

Definition 3.1. A Kähler manifold (M, g, I, ω) is called *special Kähler*, if it is equipped with a symplectic, torsion-free, flat connection ∇ such that

$$(\nabla_X I)Y = (\nabla_Y I)X \tag{3.2}$$

for all tangent vectors X and Y.

Our domain Ω can be equipped with the structure of a special Kähler manifold, which is the content of the following proposition.

Proposition 3.3. *The coordinates*

$$u = x - y + \varphi_x + \varphi_y, \ v = y - x + \varphi_x + \varphi_y$$

are isothermal for the metric g. That is, $g = e^{-\rho}(du^2 + dv^2)$, for $\rho = \log(2\varphi_{xx} + 4\varphi_{xy} + 2\varphi_{yy})$.

Additionally, the complex structure, symplectic form, and connection

$$I = -\tfrac{\partial}{\partial u} \otimes dv + \tfrac{\partial}{\partial v} \otimes du,\ \omega = g(I\cdot,\cdot),\ \nabla = d$$

give Ω *the structure of a special Kähler manifold with holomorphic coordinate* $z = u + iv$.

Proof. The proof is a computation. First,

$$\begin{aligned} du^2 + dv^2 &= ((1+\varphi_{xx}+\varphi_{xy})dx + (-1+\varphi_{xy}+\varphi_{yy})dy)^2 \\ &+ ((-1+\varphi_{xx}+\varphi_{xy})dx + (1+\varphi_{xy}+\varphi_{yy})dy)^2 \\ &= (2+2\varphi_{xx}^2+4\varphi_{xx}\varphi_{xy}+2\varphi_{xy}^2)dx^2 \\ &+ (-4+4\varphi_{xx}\varphi_{xy}+4\varphi_{xx}\varphi_{yy}+4\varphi_{xy}^2+4\varphi_{xy}\varphi_{yy})dxdy \\ &+ (2+2\varphi_{xy}^2+4\varphi_{xy}\varphi_{yy}+2\varphi_{yy}^2)dy^2 \\ &= (2\varphi_{xx}+4\varphi_{xy}+2\varphi_{yy})(\varphi_{xx}\ dx^2 + \varphi_{xy}\ dxdy + \varphi_{yy}\ dy^2) \end{aligned}$$

where in the last step we made use of $\varphi_{xx}\varphi_{yy} - \varphi_{xy}^2 = 1$. Hence,

$$g = \frac{1}{2\varphi_{xx}+4\varphi_{xy}+2\varphi_{yy}}(du^2+dv^2).$$

The definition of ω guarantees that (Ω, g, I, ω) forms a Kähler manifold. Therefore it will suffice to check that ∇ is a symplectic, torsion-free, flat connection satisfying (3.2). First, that ∇ is torsion-free and flat is immediate from the definition. To check that ∇ is symplectic, we calculate ω in (x, y) coordinates:

$$\begin{aligned} \omega &= g(I\cdot,\cdot) \\ &= \frac{1}{2\varphi_{xx}+4\varphi_{xy}+2\varphi_{yy}}(-dvdu + dudv) \\ &= \frac{du\wedge dv}{\varphi_{xx}+2\varphi_{xy}+\varphi_{yy}} \\ &= \frac{(u_x\ dx + u_y\ dy)\wedge(v_x\ dx + v_y\ dy)}{\varphi_{xx}+2\varphi_{xy}+\varphi_{yy}} \\ &= \frac{(u_xv_y - u_yv_x)dx\wedge dy}{\varphi_{xx}+2\varphi_{xy}+\varphi_{yy}} \\ &= 2\ dx\wedge dy. \end{aligned}$$

It follows then that ω is parallel with respect to ∇. Finally, to check (3.2), we express it in (x, y) coordinates. To do so, suppose

$$I = I^1\ \tfrac{\partial}{\partial x}\otimes dx + I^2\ \tfrac{\partial}{\partial x}\otimes dy + I^3\ \tfrac{\partial}{\partial y}\otimes dx + I^4\ \tfrac{\partial}{\partial y}\otimes dy.$$

Then

$$\begin{aligned} \nabla I = &I_x^1\ \tfrac{\partial}{\partial x}\otimes dx\otimes dx + I_y^1\ \tfrac{\partial}{\partial x}\otimes dy\otimes dx \\ &+ I_x^2\ \tfrac{\partial}{\partial x}\otimes dx\otimes dy + I_y^2\ \tfrac{\partial}{\partial x}\otimes dy\otimes dy \\ &+ I_x^3\ \tfrac{\partial}{\partial y}\otimes dx\otimes dx + I_y^3\ \tfrac{\partial}{\partial y}\otimes dy\otimes dx \\ &+ I_x^4\ \tfrac{\partial}{\partial y}\otimes dx\otimes dy + I_y^4\ \tfrac{\partial}{\partial y}\otimes dy\otimes dy, \end{aligned}$$

so the condition in (3.2) becomes

$$I_y^1 = I_x^2,\ I_y^3 = I_x^4.$$

Then to verify this we express I in (x, y) coordinates:

$$\begin{aligned} I &= -\tfrac{\partial}{\partial u} \otimes dv + \tfrac{\partial}{\partial v} \otimes du \\ &= -\frac{1}{u_x v_y - u_y v_x}(v_y \ \tfrac{\partial}{\partial x} - v_x \ \tfrac{\partial}{\partial y}) \otimes (v_x \ dx + v_y \ dy) \\ &+ \frac{1}{u_x v_y - u_y v_x}(-u_y \ \tfrac{\partial}{\partial x} + u_x \ \tfrac{\partial}{\partial y}) \otimes (u_x \ dx + u_y \ dy) \\ &= \frac{1}{u_x v_y - u_y v_x}[(-v_x v_y - u_x u_y)(\tfrac{\partial}{\partial x} \otimes dx) + (-v_y^2 - u_y^2)(\tfrac{\partial}{\partial x} \otimes dy) \\ &+ (v_x^2 + u_x^2)(\tfrac{\partial}{\partial y} \otimes dx) + (v_x v_y + u_x u_y)(\tfrac{\partial}{\partial y} \otimes dy)] \\ &= -\varphi_{xy} \ \tfrac{\partial}{\partial x} \otimes dx + -\varphi_{yy} \ \tfrac{\partial}{\partial x} \otimes dy + \varphi_{xx} \ \tfrac{\partial}{\partial y} \otimes dx + \varphi_{xy} \ \tfrac{\partial}{\partial y} \otimes dy, \end{aligned}$$

where we have again used the fact that $\varphi_{xx}\varphi_{yy} - \varphi_{xy}^2 = 1$. Since $\frac{\partial}{\partial y}(-\varphi_{xy}) = \frac{\partial}{\partial x}(-\varphi_{yy})$ and $\frac{\partial}{\partial y}\varphi_{xx} = \frac{\partial}{\partial x}\varphi_{xy}$, we find (3.2) is satisfied. Thus, ∇ induces a special Kähler structure on Ω. ■

We are now ready to describe how this additional structure on the domain Ω yields asymptotics for our metric g.

3.2. **Asymptotics for the conformal factor.** Special Kähler metrics on the punctured disk $B_1^* \subseteq \mathbb{C}$ of the form $g = e^{-\rho}|dz|^2$ were studied in [4] and [1] by demonstrating that every such metric has an associated metric $\tilde{g} = e^{2\rho}|dz|^2$ of non-positive Gaussian curvature. In [4], the author shows the curvature of $\tilde{g}$ is $\tilde{K} = -16|\Xi_0|^2$, where $\Xi = \Xi_0 \ dz^3$ is the holomorphic cubic form of the special Kähler metric g.

Assuming Ξ does not have an essential singularity yields a bound

$$-C_1|z|^l \leq \tilde{K} \leq -C_2|z|^l,$$

where C_1, C_2 are positive constants and $l \in \mathbb{R}$. Then, by invoking a result of [7] for the problem of prescribed non-positive Gaussian curvature, the author obtains explicit models for the conformal factor ρ at the origin, culminating in the following result.

Theorem 3.4. [4, Theorem 1.1]
Let $g = e^{-\rho}|dz|^2$ be a special Kähler metric on B_1^*. Assume that Ξ is holomorphic on the punctured disc and the order of Ξ at the origin is $n > -\infty$. Then

$$e^{-\rho} = -|z|^{n+1}\log|z|e^{O(1)} \qquad \text{or} \qquad e^{-\rho} = |z|^{\beta}(C + o(1)) \tag{3.5}$$

as $z \to 0$, where $C > 0$ and $\beta < n + 1$.

Moreover, for any $n \in \mathbb{Z}$ and $\beta \in \mathbb{R}$ such that $\beta < n+1$ there is a special Kähler metric satisfying (3.5).

In later sections we shall refer to the models of the form $-|z|^{n+1}\log|z|e^{O(1)}$ as *logarithmic* and those of the form $|z|^{\beta}(C + o(1))$ as *conic*. Additionally, we shall refer to logarithmic models of exponent $n + 1 > 0$ and conic models of exponent $\beta > 0$ as *vanishing*, while referring to logarithmic models of exponent $n + 1 \leq 0$ and conic models of exponent $\beta < 0$ as *diverging*.

We now describe how this result applies to our metric g. Recall that $g = e^{-\rho}|dz|^2$, where $\rho = \log(2\varphi_{xx} + 4\varphi_{xy} + 2\varphi_{yy})$. Supposing that ρ is C^2 on a disc around the

origin and Ξ_0 is nonessential, we find

$$\frac{1}{2\varphi_{xx}+4\varphi_{xy}+2\varphi_{yy}} = \begin{cases} -|z|^{n+1}\log|z|e^{O(1)} \\ |z|^{\beta}(C+o(1)) \end{cases}$$

and therefore

$$\varphi_{xx}+2\varphi_{xy}+\varphi_{yy} = \begin{cases} -\frac{e^{O(1)}}{|z|^{n+1}\log|z|} \\ |z|^{-\beta}(C+o(1)). \end{cases}$$

What we will see is that only a single model is compatible with the boundedness of $D^2\varphi$ up to the origin, that being the conic singularity with exponent $\beta = 0$. In the appendix we describe a heuristic for disregarding this case based on the impossibility of complete special Kähler metric on the sphere.

3.3. **Consequences for regularity of the transport map.** We are now ready to prove Theorem 1.1.

Proof. First, if we have a vanishing model for $e^{-\rho}$, then $\varphi_{xx}+2\varphi_{xy}+\varphi_{yy}$ diverges at the origin, which implies that at least one of φ_{xx}, φ_{xy}, or φ_{yy} diverges there as well.

Second, if we have a diverging model for $e^{-\rho}$, then $\varphi_{xx}+2\varphi_{xy}+\varphi_{yy}$ vanishes at the origin. Suppose toward a contradiction that $|D^2\varphi| \leq M$ and we have a diverging model for $e^{-\rho}$, i.e.

$$\varphi_{xx}+2\varphi_{xy}+\varphi_{yy} = o(1).$$

Then

$$\varphi_{xy}^2 = \frac{\varphi_{xx}^2+2\varphi_{xx}\varphi_{yy}+\varphi_{yy}^2}{4} + o(1)(\varphi_{xx}+\varphi_{yy}) + o(1).$$

Since $|\varphi_{xx}+\varphi_{yy}| \leq 2M$, this is to say

$$\varphi_{xy}^2 = \frac{\varphi_{xx}^2+2\varphi_{xx}\varphi_{yy}+\varphi_{yy}^2}{4} + o(1).$$

Therefore we find

$$\begin{aligned} \varphi_{xx}\varphi_{yy}-\varphi_{xy}^2 &= -\tfrac{1}{4}\varphi_{xx}^2+\tfrac{1}{2}\varphi_{xx}\varphi_{yy}-\tfrac{1}{4}\varphi_{yy}^2+o(1) \\ &= -\tfrac{1}{4}(\varphi_{xx}-\varphi_{yy})^2+o(1), \end{aligned}$$

which violates the Monge-Ampère equation $\varphi_{xx}\varphi_{yy}-\varphi_{xy}^2 = 1$ in some neighborhood of the origin.

We conclude that $|D^2\varphi|$ is unbounded in every case but conic with $\beta = 0$. ∎

4. Numerical Investigations

To get an idea of the model for our metric, we numerically simulate the optimal transport problem, and then compute the related quantities.

To effectively approximate our transport map, we discretize the Monge problem associated to the planar optimal transport problem. Because our measures on both domains are Lebesgue measure, we instead solve the assignment problem using the SciPy implementation of the Jonker-Volgenant algorithm. This was done by first fixing a grid of points on our source domain. Then we fix the same number points on the target domain randomly. Running the assignment algorithm generates a pairing of points in the source to points in the target.

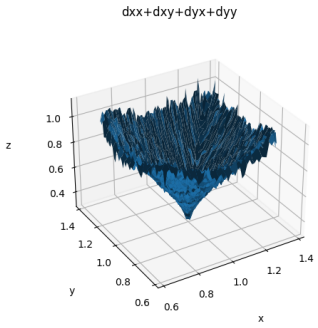

FIGURE 4. A graph of e^{ρ} in u, v coordinates.

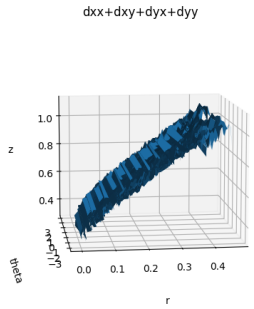

FIGURE 5. Graph of e^{ρ} in polar u, v coords.

The process just described constitutes one trial. Keeping the source grid fixed and repeating these trials for many random grids yields a list of values for the transport map at each grid point. By averaging these values we improve the regularity of the components; in particular we obtain a transport map whose components are better suited for taking numerical derivatives than if we had fixed a grid in the target domain.

We then graph e^{ρ} in u, v coordinates, which we notice is roughly radial, as depicted in Figure A. This motivates writing e^{ρ} in polar coordinates around the singular point, i.e. by setting $r = \sqrt{u^2 + v^2}, \theta = \arctan(\frac{v}{u})$. Ignoring the parameter θ, we may plot our data in a scatterplot of e^{ρ} against r, and begin to compare this to the radial estimates provided by [1]. We notice that the only logarithmic model which approximates our data well is the case $n = -1$. Conical models which approximate the data are roughly those satisfying $0 < \beta < 0.2$.

APPENDIX A. DISCUSSION OF REGULARITY FOR ρ AND Ξ

It is not clear that our choice of coordinates yields a conformal factor that is C^2 in a neighborhood of the origin, nor is it clear that the holomorphic cubic form associated to g does not have an essential singularity at the origin. Here we will discuss some outlooks on the resolution of these two problems.

Our metric g is grossly discontinuous in (x, y) coordinates across the ray $\{(t, t) \mid t > 0\}$. This is a result of the non-convexity of the target domain, which results in the transport map sending opposite sides of the ray to points which are far apart. Our choice of u and v begin to remediate this concern. Namely, the factor ρ is symmetric about the line $y = x$, and is continuous barring divergence or oscillation (neither of which are witnessed in numerical simulations). We continue to investigate if ρ is differentiable in u, v coordinates.

If Ξ_0 has an essential singularity at the origin, then the image of any disc around the origin is dense in $\mathbb{C}$. Knowing that $\tilde{K} = -16|\Xi_0|^2$, we can obtain an explicit formula for this modulus as follows.

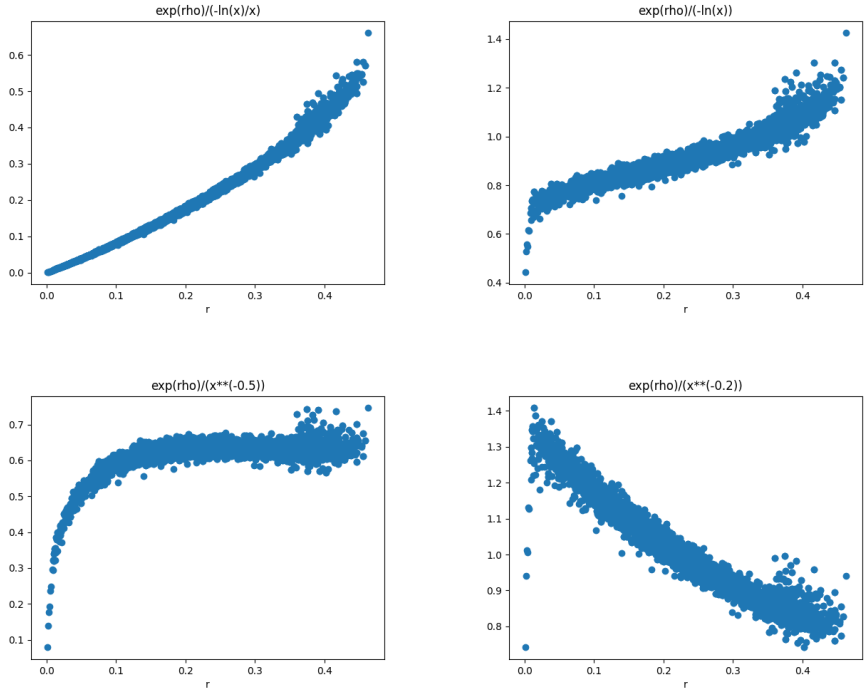

The Gaussian curvature of a metric $g = E\ dx^2 + F(dxdy + dydx) + G\ dy^2$ is given by the formula

$$K = \frac{\begin{vmatrix} -\frac{1}{2}E_{yy} + F_{xy} - \frac{1}{2}G_{xx} & \frac{1}{2}E_x & F_x - \frac{1}{2}E_y \\ F_y - \frac{1}{2}G_x & E & F \\ \frac{1}{2}G_y & F & G \end{vmatrix} - \begin{vmatrix} 0 & \frac{1}{2}E_y & \frac{1}{2}G_x \\ \frac{1}{2}E_y & E & F \\ \frac{1}{2}G_x & F & G \end{vmatrix}}{(EG - F^2)^2}.$$

For the metric $g = e^{-\rho}(du^2 + dv^2) = \varphi_{xx}\ dx^2 + \varphi_{xy}(dxdy + dydx) + \varphi_{yy}\ dy^2$, this is

$$K = \begin{vmatrix} 0 & \frac{1}{2}\varphi_{xxx} & \frac{1}{2}\varphi_{xxy} \\ \frac{1}{2}\varphi_{xyy} & \varphi_{xx} & \varphi_{xy} \\ \frac{1}{2}\varphi_{yyy} & \varphi_{xy} & \varphi_{yy} \end{vmatrix} - \begin{vmatrix} 0 & \frac{1}{2}\varphi_{xxy} & \frac{1}{2}\varphi_{xyy} \\ \frac{1}{2}\varphi_{xxy} & \varphi_{xx} & \varphi_{xy} \\ \frac{1}{2}\varphi_{xyy} & \varphi_{xy} & \varphi_{yy} \end{vmatrix}$$

$$K = -\frac{\varphi_{xx}}{4}(\varphi_{xxy}\varphi_{yyy} + \varphi_{xyy}^2) - \frac{\varphi_{yy}}{4}(\varphi_{xyy}\varphi_{xxx} + \varphi_{xxy}^2) + \frac{\varphi_{xy}}{4}(\varphi_{xxx}\varphi_{yyy} + 3\varphi_{xxy}\varphi_{xyy})$$

Then, by differentiating the Monge-Ampère equation with respect to x and y, we find

$$\varphi_{xxx}\varphi_{yy} + \varphi_{xx}\varphi_{xyy} - 2\varphi_{xy}\varphi_{xxy} = 0,\ \ \varphi_{xx}\varphi_{yyy} + \varphi_{xxy}\varphi_{yy} - 2\varphi_{xy}\varphi_{xyy} = 0.$$

Which implies

$$K = \frac{\varphi_{xy}}{4}(\varphi_{xxx}\varphi_{yyy} - \varphi_{xxy}\varphi_{xyy}).$$

Then by

$$K = \frac{e^{\rho}}{2}\Delta\rho,\ \ \tilde{K} = -e^{-2\rho}\Delta\rho,$$

we find

$$|\Xi_0|^2 = -\frac{1}{16}\tilde{K} = \frac{1}{8}e^{-3\rho}K = \frac{\varphi_{xy}(\varphi_{xxx}\varphi_{yyy} - \varphi_{xxy}\varphi_{xyy})}{256(\varphi_{xx} + 2\varphi_{xy} + \varphi_{yy})^3}.$$

If we can bound this quantity away from any value, then we can conclude Ξ_0 does not have an essential singularity at the origin.

Appendix B. The case $\beta = 0$

As proved by Lu in [6], the only complete special Kähler structures are flat. This gives a strong indication that the case of $\beta = 0$ mentioned previously should be impossible. Indeed, supposing that $e^{-\rho}$ has a conic model at the origin with $\beta = 0$, we would find that the metric g is continuous in (u, v) coordinates. Then the (u, v) coordinate change is continuous: u and v are symmetric about $x = y$, and we have uniform continuity of φ_x and φ_y from standard regularity results in optimal transport. Since this coordinate change is continuous, we find that g is indeed a metric on all of Ω.

Since φ is symmetric on the surface of the simplex, we find that g is continuous over every singularity. In particular, we find that we are able to extend our special Kähler structure to the entire surface of the simplex, which has the topology of the 2-sphere. However, a complete special Kähler metric is flat, which implies that we have constructed a flat metric on the entire 2-sphere, a contradiction. Thus, the case of $\beta = 0$ is seen to be impossible.

Acknowledgments

The authors thank their mentors Mattias Jonsson and Nicholas McCleerey for their generous help throughout the University of Michigan's 2023 Summer REU program.

References

[1] Martin Callies and Andriy Haydys. Local models of isolated singularities for affine special kähler structures in dimension two. *International Mathematics Research Notices*, 2020(17):5215–5235, 2018.

[2] A. Figalli and F. Glaudo. *An Invitation to Optimal Transport, Wasserstein Distances, and Gradient Flows*. EMS Press, Aug 2021.

[3] Daniel S. Freed. Special kähler manifolds. *Communications in Mathematical Physics*, 203(1):31–52, May 1999.

[4] Andriy Haydys. Isolated singularities of affine special kähler metrics in two dimensions. *Communications in Mathematical Physics*, 340(3):1231–1237, 2015.

[5] Jakob Hultgren, Mattias Jonsson, Enrica Mazzon, and Nicholas McCleerey. Tropical and non-archimedean monge-ampère equations for a class of calabi-yau hypersurfaces, 2023.

[6] Zhiqin Lu. A note on special kähler manifolds. *Mathematische Annalen*, 313(4):711–713, Apr 1999.

[7] R.C. McOwen. Prescribed curvature and singularities of conformal metrics on riemann surfaces. *Journal of Mathematical Analysis and Applications*, 177(1):287–298, 1993.

[8] Gabriel Peyré and Marco Cuturi. *Computational Optimal Transport*. 2020.